CRYSTAL GROWTH & DESIGN

Communication

Cite This: *Cryst. Growth Des.* 2019, 19, 6011−6016

pubs.acs.org/crystal

DMAP-Induced Gallium Phosphites with Different Dimensionality

Cong Lin,[†,‡] Jian Li,[†] Yan Wang,[‡] Diming Xu,[†] Fuhui Liao,[†] Jianhua Lin,[†] Feng Pan,*[,‡] and Junliang Sun*[,†]

[†]College of Chemistry and Molecular Engineering, Peking University, Beijing 100871, China

[‡]School of Advanced Materials, Shenzhen Graduate School, Peking University, Shenzhen 518055, China

Supporting Information

ABSTRACT: Three novel gallium phosphites, **Ga-3**, **Ga-2**, and **Ga-1**, have been hydrothermally synthesized via the commercial 4-dimethylaminopyridine (DMAP) reagent serving as a template in **Ga-3** and **Ga-1** and a ligand in **Ga-2**. These main-group-metal phosphites present different topology from the first 3D framework containing extra-large 14-ring (14R) channel (**Ga-3**) and then the second 2D organic−inorganic hybrid layer (**Ga-2**) to the first 1D gallium phosphite chain (**Ga-1**). The structure detail of the three compounds, examined by single-crystal X-ray diffraction (SXRD), is discussed to elucidate the topology difference.

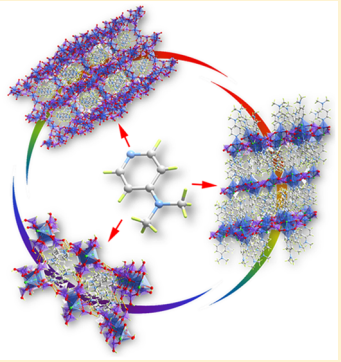

Inorganic open-framework materials, typically zeolites and metal phosphate molecular sieves, have been extensively explored and utilized in various conventional gas separation, ion exchange, and catalysis processes.[1−4] An important extension of the metal phosphate molecular sieve materials is the metal phosphites achieved by replacing the anionic $[PO_4]^{3-}$ tetrahedra with $[HPO_3]^{2-}$ pseudopyramids, which have already attracted particular research interest due to their diverse framework structures as well as novel properties such as magnetism, fluorescence, and H_2 and CO_2 storage.[5−8] Notably, the P−H tails in the pseudopyramidal $[HPO_3]^{2-}$ groups could greatly affect their linkages with the metal ions; this results in the tendency to form exceptional interrupted open-framework structures with extra-large channels (pore size larger than 12R) beneficial to the potential applications on large molecules.[9−11] Until now, numerous extra-large-channel metal phosphites have been accquired, for example, Cr-NKU-24 with 24R channels,[12] NTHU-5 with 26R channels,[13] and NTHU-13 with 24R to 72R channels.[14] Nevertheless, almost all of these metal phosphites with extra-large channels contain the transiton-metal participants in their frameworks, also leading to the largest number of phosphite structures. In sharp contrast is the study into the pure main-group-metal phosphites, which still remain seriously insufficient with much fewer kinds and smaller channels.[15−17]

Although only a very limited number of open-framework gallium phosphites with 10R or 12R channels have been reported in the last 30 years,[18−25] unfortunately, there is only one extra-large-channel gallium phosphite so far, i.e., NTHU-15 with 18R channels.[8] Moreover, besides those small number of 3D open-framework members mentioned above, the gallium phosphites with lower dimensions, such as the 2D layers and 1D chains, are even more scarce. Actually, in the gallium phosphite system, there are only two reported 2D structures,[26,27] but no 1D materials have ever been achieved. Consequently, there still remains a great challenge to acquire the novel gallium phosphites with more structure types as well as different dimensionality, especially those with extra-large channels, 2D or 1D structures, which are of significance for the materials as well as structural chemistry of the metal phosphite family.

On the other hand, it is well-known that the organic structure-directing agents (OSDA) with versatile functions play the most crucial role in the synthesis of open-framework materials.[1,3] Although the commercial DMAP reagent has already been reported to template several novel open-framework structures, such as the aluminophosphate SSZ-51 and the germanosilicate IM-18 and PKU-16,[28−30] it has never led to 1D chained structures nor been utilized in the metal phosphite system. Until recently, it was employed as the OSDA to construct a 14R-channel aluminophosphite PKU-25Al, indicating its feasibility in synthesizing the main-group-metal phosphites.[31] Thus, following this idea, by introducing the DMAP ingredient into the gallium phosphite system for the first time, we herein report three novel various dimensional gallium phosphites with distinct structures, i.e., the first 3D extra-large 14R-channel **Ga-3** ($[(C_7H_{11}N_2)(H_3O)_{0.33}][Ga_3(HPO_3)_{4.67}(OH)(H_2O)_2]$), the second 2D organic−inorganic hybrid layered **Ga-2** ($(C_7H_{10}N_2)GaF(HPO_3)$), and the first 1D chained **Ga-1** ($[C_7H_{11}N_2]_3[(GaF)_3(H_{1.5}PO_3)_6]$).

Received: June 7, 2019
Revised: September 19, 2019
Published: September 25, 2019

DOI: 10.1021/acs.cgd.9b00725
Cryst. Growth Des. 2019, 19, 6011−6016

Ga-3, **Ga-2**, and **Ga-1** are all hydrothermally synthesized from the mixtures containing raw materials with different ratios in the Teflon-lined stainless autoclaves at 433 K for 5 days (see Supporting Information for synthesis details). **Ga-3** and **Ga-1** have been prepared as pure phases, but unfortunately, the minor Ga_2O_3 reactant exists as the impurity in the **Ga-2** product (Figure S5). Structural analyses by SXRD reveal that **Ga-3**, **Ga-2**, and **Ga-1** crystallize in the $P\bar{3}1c$, $R\bar{3}$, and $P\bar{1}$ space group, respectively (see Supporting Information for structure details, Table S1), and thus the resultant crystals exhibit hexagonal plate morphology for **Ga-3** and **Ga-2** and rod morphology for **Ga-1** (Figure S6). Consequentially, the various dimensional crystal structures of **Ga-3**, **Ga-2**, and **Ga-1** are thus determined, all of which possess structures constructed from the Ga-based octahedra, the pseudopyramidal phosphite groups, and the organic DMAP molecules. The bond lengths of the inorganic species in **Ga-3**, **Ga-2**, and **Ga-1** all agree well with those from other gallium phosphites.[8,18−27]

Ga-3 possesses a 3D open-framework structure, almost consistent with the previously reported PKU-25Al from their similar powder X-ray diffraction patterns (PXRD) (Figure S5).[31] The asymmetric unit of **Ga-3** is shown in Figure S1a. Similarly, the 5-connected GaO_6 octahedra and the $[HPO_3]^{2-}$ groups are first alternately connected to construct the ABAB stacked *hcb* layers with 12R in the *ab* plane.[31−33] The bonding of the 4- and 6-connected GaO_6 octahedra with the $[HPO_3]^{2-}$ groups constitutes the particular chains with unprecedented face-sharing GaO_6 octahedra dimers formed by three −O(9)H groups connecting two Ga(3) atoms along the *c*-axis (Figure 1a and b), as verified by the SXRD refinement (Figure 1d) and the bond valence sum (BVS) calculations. Meanwhile, apart from PKU-25Al, no obvious structural disorder of the face-sharing GaO_6 octahedra dimers in **Ga-3** is observed from the SXRD refinement.[31] Although the bonding of two Ga atoms by −OH groups has been reported previously,[22,25] it has only led to the formation of corner-sharing GaO_6 octahedra. Consequently, such face-sharing GaO_6 octahedra dimers are very rare, and have appeared in another relatively dense gallium phosphite.[19]

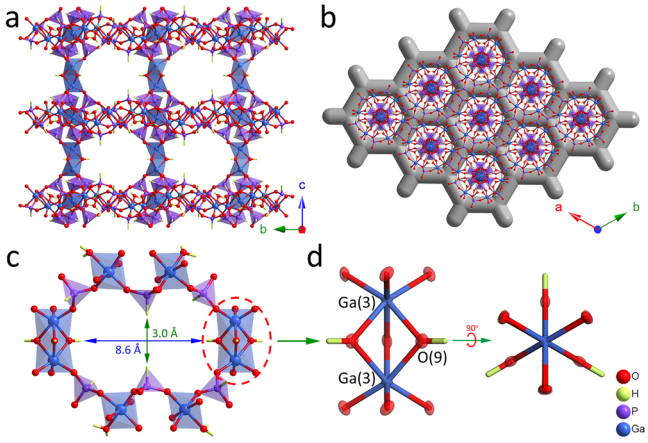

Figure 1. Crystal structure of **Ga-3**. (a) 3D open-framework structure. (b) 2D honeycomb-like 14R-channel system shown as dark gray sticks. (c) Dumbbell-shaped 14R-channel window. (d) Unprecedented face-sharing GaO_6 octahedra dimer with 50% probability.

Eventually, by stringing the gallium phosphite layers via the chains through the 12R, the 3D inorganic open-framework structure of **Ga-3** is therefore accomplished with a distinct topology (Figure 1a), in which a 2D honeycomb-like extra-large 14R-channel system running in the *ab* plane is also achieved (Figure 1b). To the best of our knowledge, **Ga-3** is the first gallium phosphite with extra-large 14R channels, whose dumbbell-shaped channel window is shown in Figure 1c. Meanwhile, the particular 9/14 ratio of Ga/P in **Ga-3** is also obtained in a single phase for the first time.[8,18−27,34−39] Similar to PKU-25Al, numerous clover-like chiral 4═1 units (Figure S2a) as well as chiral channel motifs (Figure S2b) also exist and are alternately arranged.[31] The protonated DMAP molecules reside in a disordered arrangement in the locations near the 14R-channel windows and interact with each other and the inorganic framework through $\pi-\pi$ interaction and hydrogen bonding, respectively (Figure S2c),[31] which are further distributed in the channel voids of **Ga-3** with a rare triangular pattern (Figure S2d).

With respect to **Ga-2**, it exhibits a 2D hybrid layered structure. The asymmetric unit of **Ga-2** is shown in Figure S1b. Every Ga atom is first coordinated with three O atoms from three $[HPO_3]^{2-}$ groups, two F atoms, and one N atom from the pyridine ring of the DMAP molecule, resulting in the novel hybrid 4-connected GaO_3F_2N octahedron and further the $GaO_3F_2(C_7H_{10}N_2)$ unit, while all the $[HPO_3]^{2-}$ groups are still 3-connected with three GaO_3F_2N octahedra. The hybrid $GaO_3F_2(C_7H_{10}N_2)$ units are then corner-shared with the $[HPO_3]^{2-}$ groups via the bridge O atoms and edge-shared with the other $GaO_3F_2(C_7H_{10}N_2)$ units via the bridge F atoms to construct the unique single organic−inorganic hybrid layer (Figure 2c). Such layers could also be considered to be constituted separately by two kinds of independent SBU. One is designated as SBU-1 with 3-connectivity and generated by the alternate corner-sharing of three $GaO_3F_2(C_7H_{10}N_2)$ units with three $[HPO_3]^{2-}$ groups, further leading to the 6R (Figure 2a). Meanwhile, the three DMAP molecules in every SBU-1 are on the same side and almost perpendicular to the 6R, interact with each other via the T-shaped $\pi-\pi$ interaction,[40] and later form two kinds of three-leaf windmill-like trimers with opposite configurations (Figure 2a and Figure S3a). As is known to all, the aromatic DMAP molecules usually adopt the $\pi-\pi$ stacked mode to reside in materials,[28,40−42] while other special existences, such as the triangular arrangement in **Ga-3** (Figure S 2d) and PKU-25Al or existing as an individual in IM-18,[30,31] have also been reported. However, no such three-leaf windmill-like trimers of the DMAP molecules in **Ga-2** have ever been observed (Figure S3a). The other SBU, denoted as SBU-1′ with 4-connectivity, is acquired directly by bonding two edge-sharing $GaO_3F_2(C_7H_{10}N_2)$ units and two $[HPO_3]^{2-}$ groups, in which the two DMAP molecules are on the opposite sides, as shown in Figure 2b.

Subsequently, adjacent SBU-1 with the opposite configurations of the three-leaf windmill-like DMAP trimers stretch to the opposite directions and are connected via corner- and edge-sharing, leading to the single hybrid layer of **Ga-2** in the *ab* plane with 6R and large 12R encircled by the alternate six octahedra and six pseudopyramides (Figure 2c). Meanwhile, such a layer could also be constructed alone by the corner-sharing of SBU-1′. Further simplifying the layer structure would result in the *hcb* (6^3 net) or *kgm* (kagomé net) topology when separately considering SBU-1 or SBU-1′ as the node (shown respectively in Figure 2d as the purple or yellow lattice).[31−33] Later, the hybrid layers are ABCABC arranged along the *c*-axis with their DMAP trimers stretching to the 12R

DOI: 10.1021/acs.cgd.9b00725
Cryst. Growth Des. 2019, 19, 6011−6016

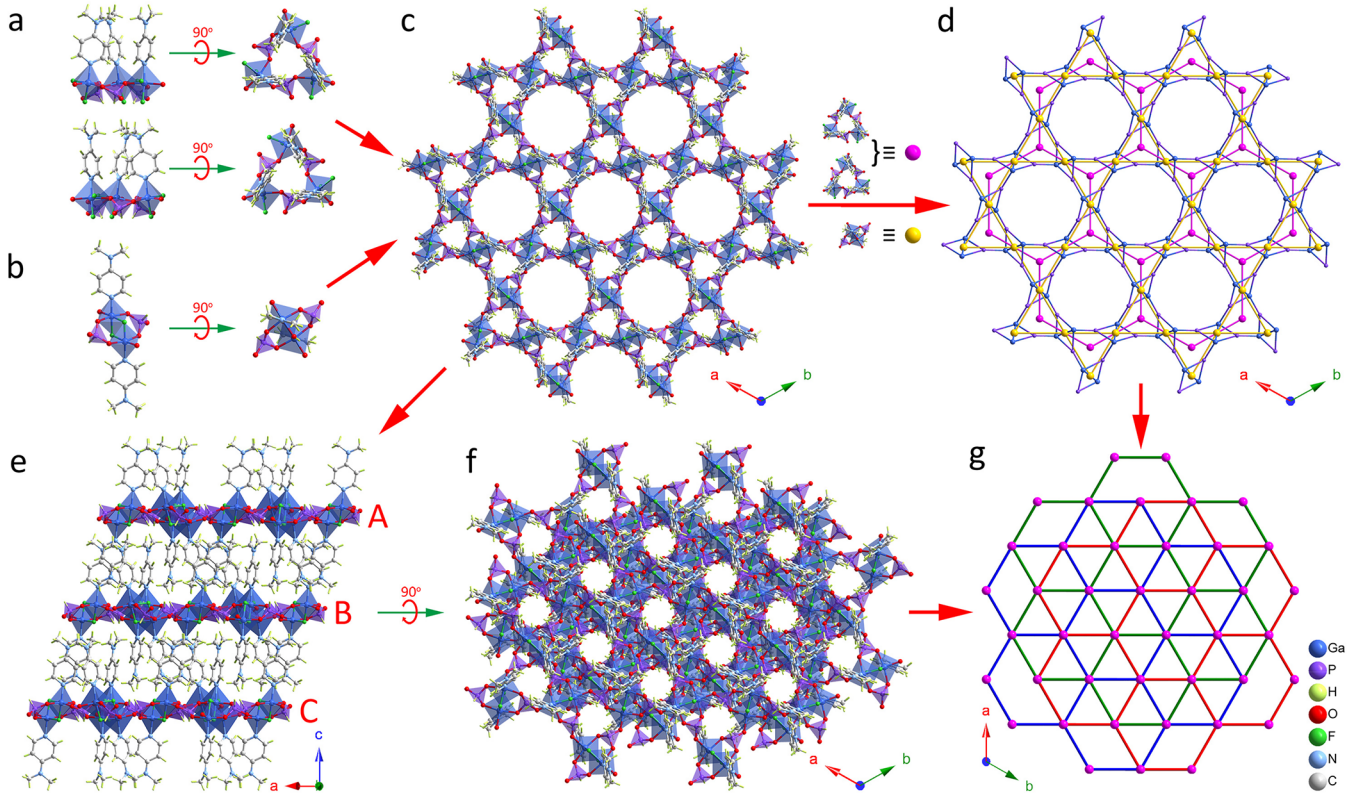

Figure 2. Crystal structure of **Ga-2**. (a) SBU-1 with opposite configurations of three-leaf windmill-like DMAP trimers. (b) SBU-1′. (c) Single hybrid layer with large 12R. (d) Layer topology with the *hcb* and *kgm* net shown, respectively, in the purple and yellow lattice. The accumulated layered structures viewed along the *b*- and *c*-axis are shown in (e) and (f), respectively. (g) Layer accumulation pattern shown by the *hcb* topology with the red, green, and blue lattice representing the layers from top to bottom along the *c*-axis.

of the adjacent layers. In the meantime, the $\pi-\pi$ stacking interactions between the DMAP molecules from neighboring layers are also formed, which integrate all the hybrid layers and generate a complex arrangement pattern of the DMAP molecules (Figure S3b). As a result, the unique layered structure of **Ga-2** with inaccessible small 6R channels along the *c*-axis is achieved (Figure 2e and f). The layer accumulation pattern is also analyzed by the *hcb* topology and reminiscent of the famous multilayer graphene (Figure 2g). Up to now, there is only one organic−inorganic hybrid gallium phosphite; thus, **Ga-2** is the second hybrid and also the third layered gallium phosphite with an exceptional structure.[26,27]

As for **Ga-1**, it is a 1D gallium phosphite with a chained structure. The asymmetric unit of **Ga-1** is shown in Figure S1c. All the Ga atoms are bonded with four O atoms from four $[H_{1.5}PO_3]^{1.5-}$ groups and two F atoms, leading to the 6-connected GaO_4F_2 octahedra, while all the $[H_{1.5}PO_3]^{1.5-}$ groups are 2-connected. Such low connectivity of the pseudopyramidal phosphite groups is very rare, since it has only been observed in two aluminophosphites.[43] Meanwhile, it is worth mentioning that each phosphite group in **Ga-1** possesses a terminal −OH with 0.5 occupancy of the H atom, as indicated by the SXRD refinement, charge balance, and element analysis (EA, Table S3), thus resulting in the formula of $[H_{1.5}PO_3]^{1.5-}$. Each GaO_4F_2 octahedron first corner-shares with each other via the bridge F atoms to form a unique Ga−F−Ga chain (Figure S4). Although the Ga−F−Ga connection has been reported in several gallophosphates and gallium phosphites,[22,25,27,44,45] such an infinite Ga−F−Ga chain in **Ga-1** is very rare and has only been discovered in one fluorogallophosphate.[46] Subsequently, the $[H_{1.5}PO_3]^{1.5-}$ groups connect two adjacent GaO_4F_2 octahedra, and the gallium phosphite chains with the formula $[(GaF)(H_{1.5}PO_3)_2]^-$ are thus accomplished. These chains are further arranged parallel along the [011] direction (Figure 3). Every two protonated DMAP molecules with their N-dimethyl groups stretching to the opposite directions are then $\pi-\pi$ stacked in the interchain voids, leading to the uncommon DMAP dimers.[28,31,40−42] Finally, the 1D chained structure of

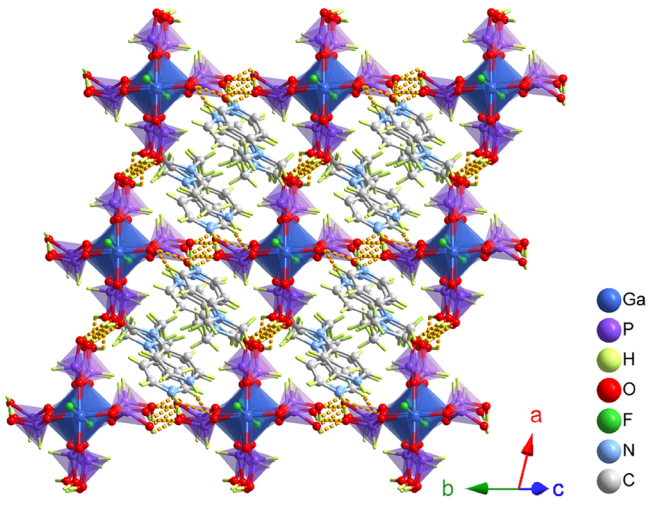

Figure 3. Crystal structure of **Ga-1** viewed along the [011] direction with the hydrogen bonds shown in the orange dashed line.

DOI: 10.1021/acs.cgd.9b00725
Cryst. Growth Des. 2019, 19, 6011−6016

Ga-1 is therefore achieved (Figure 3), which is also the first 1D gallium phosphite and the first 1D material templated by DMAP.

Another distinctive feature of the **Ga-1** structure is the presence of a large number of hydrogen bonds (Table S2). Every DMAP molecule interacts with the O atoms of the gallium phosphite chains via the protonated pyridine N atoms, thus linking the organic and inorganic species; the gallium phosphite chains are hydrogen bonded with each other via the terminal −OH groups. Therefore, a 3D hydrogen-bonding network is constructed by the gallium phosphite chains in the **Ga-1** structure, resulting in a pseudoporous hydrogen-bonding framework with multidimensional 12R channels along the [011] direction (Figure 3) and 8R channels along the *a*- and *b*-axes as well as [0$\bar{2}$1] and [311] directions (Figure S4). Such abundant hydrogen-bonding interactions have been rarely observed in inorganic materials,[47,48] indicating the uniqueness of the **Ga-1** structure, which are also vital for the structure stabilization of **Ga-1**.

As described above, **Ga-3**, **Ga-2**, and **Ga-1** all possess quite special architectures with different dimensionality. Since they are prepared under the same temperature and time, it is the raw materials as well as their ratios that play the remarkable roles in the formation of these diverse compounds. First, although the absence of the HF mineralizer may affect the crystallinity of **Ga-3**, it is indispensable for **Ga-2** and **Ga-1** due to the participation of the F^- ions in their inherent structures. For instance, decreasing the HF amount seriously hinders the crystallization process of the **Ga-2** products (Figure 4b). Meanwhile, the various structural dimensions of **Ga-3**, **Ga-2**, and **Ga-1** are obviously related to the different ratios of gallium, phosphorous acid, and DMAP. On the basis of the **Ga-3** preparation, increasing the amounts of phosphorous acid or DMAP gradually reduces the resultants' dimension from the 3D **Ga-3** to the 1D **Ga-1**, and the phosphorous acid is rather dominant in such a transformation (Figure 4a). As for **Ga-2** using a different gallium source, although no **Ga-3** or **Ga-1** has been observed in its preparation, more phosphorous acid or DMAP also interfers with the crystallization process, leading to the low crystallinity of **Ga-2** with some unknown impurites to which more DMAP is favorable (Figure 4b). Previous studies have reported that the ratios of raw materials seriously affect the precursor gel due to the chemical equilibrium.[31,41] Thus, it is concluded that the excess gallium and phosphite groups also greatly suppress the condensation reactions between the gallium and phosphite groups at the very early stages, while the excess $\pi-\pi$ interacting DMAP molecules occupying a large interspace can also prevent the inorganic components from coming close enough to condense. These factors contribute effectively to the transformation between **Ga-3** and **Ga-1** and the changes in the crystallinity and phases of **Ga-2**, thus affecting the products' dimensions. Such results are also meaningful for the synthesis of novel metal phosphites.

The EA results confirm the intactness of the DMAP molecules, the validity of the **Ga-3** and **Ga-1** formulas, and the amount of the Ga_2O_3 impurity in **Ga-2** (see Supporting Information for characterization details, Table S3). The thermogravimetric-differential scanning calorimetry (TG-DSC) combined with *in situ* variable temperature PXRD characterizations suggest that **Ga-3**, **Ga-2**, and **Ga-1** are thermally stable below the temperature of 503, 553, and 463 K, respectively, above which the organic DMAP molecules would decompose and/or evaporate, further leading to the structure collapse (see Supporting Information for characterization details, Figure S7). The fluorescence spectra of the DMAP solid, **Ga-3**, **Ga-2**, and **Ga-1** are basically identical and derived from the DMAP molecules (Figure S8); the Fourier transform infrared spectroscopy (FT-IR) verifies the existence of the P−H bonds in **Ga-3**, **Ga-2**, and **Ga-1** (Figure S9).[24,31,41]

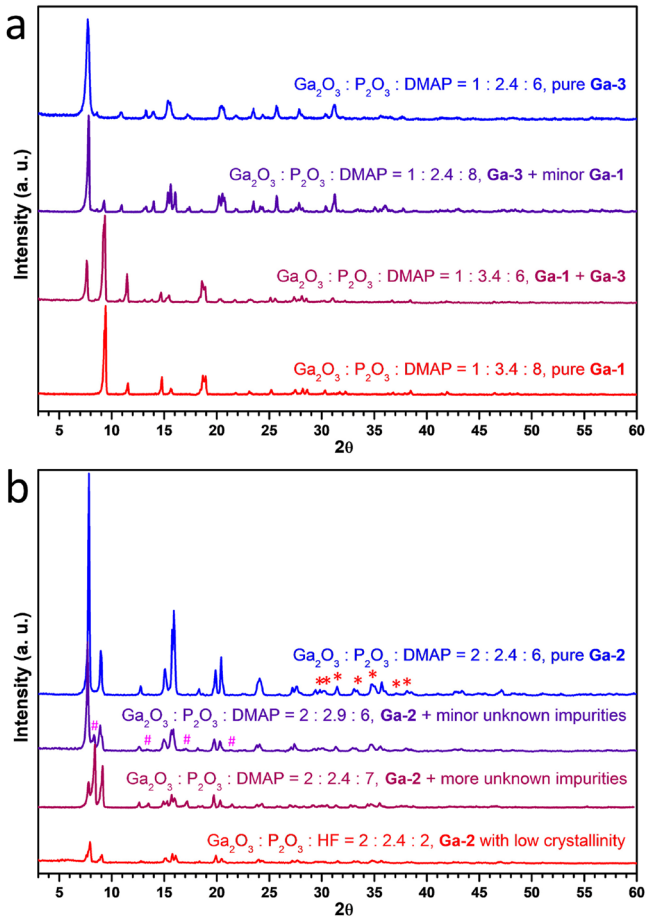

Figure 4. Synthesis explorations of **Ga-3** and **Ga-1** (a) and **Ga-2** (b). The amount of gallium and phosphorous acid is shown by their oxide forms, while the peaks marked with red asterisks (*) and purple pound keys (#) in (b) are attributed to the Ga_2O_3 and unknown impurities, respectively.

In conclusion, three novel gallium phosphites with exceptional structures, including the first extra-large 14R-channel **Ga-3**, the second organic−inorganic hybrid layered **Ga-2**, and the first chained **Ga-1**, are hydrothermally induced by the same DMAP reagent. Their syntheses, structures, and properties are discussed and characterized in detail. The compounds described here not only extend the materials chemistry for the main-group-metal phosphite family but also demonstrate the potential versatile templating effect of the commercial DMAP reagent for various dimensional materials. Further applying the DMAP template to the preparation of other metal phosphites and phosphates is thus promising and in progress.

■ ASSOCIATED CONTENT

Supporting Information

The Supporting Information is available free of charge on the ACS Publications website at DOI: 10.1021/acs.cgd.9b00725.

DOI: 10.1021/acs.cgd.9b00725
Cryst. Growth Des. 2019, 19, 6011−6016

Details of the syntheses, structures, and characterizations of **Ga-3**, **Ga-2**, and **Ga-1**, including Figures S1−S9 and Tables S1−S3 (PDF)

Accession Codes

CCDC 1879408 and 1879410−1879411 contain the supplementary crystallographic data for this paper. These data can be obtained free of charge via www.ccdc.cam.ac.uk/data_request/cif, or by emailing data_request@ccdc.cam.ac.uk, or by contacting The Cambridge Crystallographic Data Centre, 12 Union Road, Cambridge CB2 1EZ, UK; fax: +44 1223 336033.

AUTHOR INFORMATION

Corresponding Authors

*E-mail: junliang.sun@pku.edu.cn.
*E-mail: panfeng@pkusz.edu.cn.

ORCID

Feng Pan: 0000-0002-8216-1339
Junliang Sun: 0000-0003-4074-0962

Notes

The authors declare no competing financial interest.

ACKNOWLEDGMENTS

This work was supported by the National Basic Research Program of China (Nos. 2013CB933402, 2016YFA0301004), National Natural Science Foundation of China (Nos. 21671028, 21527803, 21471009, 21321001), and Soft Science Research Project of Guangdong Province (No. 2017B030301013).

REFERENCES

(1) Wang, Z.; Yu, J.; Xu, R. Needs and Trends in Rational Synthesis of Zeolitic Materials. *Chem. Soc. Rev.* **2012**, *41*, 1729−1741.

(2) Corma, A. From Microporous to Mesoporous Molecular Sieve Materials and Their Use in Catalysis. *Chem. Rev.* **1997**, *97*, 2373−2420.

(3) Simancas, R.; Dari, D.; Velamazán, N.; Navarro, M. T.; Cantín, A.; Jordá, J. L.; Satre, G.; Corma, A.; Rey, F. Modular Organic Structure-Directing Agents for the Synthesis of Zeolites. *Science* **2010**, *330*, 1219−1222.

(4) Bereciartua, P. J.; Cantín, Á.; Corma, A.; Jordá, J. L.; Palomino, M.; Rey, F.; Valencia, S.; Corcoran, E. W.; Kortunov, P.; Ravikovitch, P. I.; Burton, A.; Yoon, C.; Wang, Y.; Paur, C.; Guzman, J.; Bishop, A. R.; Casty, G. L. Control of Zeolite Framework Flexibility and Pore Topology for Separation of Ethane and Ethylene. *Science* **2017**, *358*, 1068−1071.

(5) Xing, H.; Yang, W.; Su, T.; Li, Y.; Xu, J.; Nakano, T.; Yu, J.; Xu, R. Ionothermal Synthesis of Extra-Large-Pore Open-Framework Nickel Phosphite $5H_3O{\cdot}[Ni_8(HPO_3)_9Cl_3]{\cdot}1.5H_2O$: Magnetic Anisotropy of the Antiferromagnetism. *Angew. Chem., Int. Ed.* **2010**, *49*, 2328−2331.

(6) Jhang, P.-C.; Yang, Y.-C.; Lai, Y.-C.; Liu, W.-R.; Wang, S.-L. A Fully Integrated Nanotubular Yellow-Green Phosphor from an Environmentally Friendly Eutectic Solvent. *Angew. Chem.* **2009**, *121*, 756−759.

(7) Huang, H.-L.; Wang, S.-L. Nanoribbon-Structured Organo Zinc Phosphite Polymorphs with White-Light Photoluminescence. *Angew. Chem., Int. Ed.* **2015**, *54*, 965−968.

(8) Sie, M.-J.; Lin, C.-H.; Wang, S.-L. Polyamine-Cladded 18-Ring-Channel Gallium Phosphites with High-Capacity Hydrogen Adsorption and Carbon Dioxide Capture. *J. Am. Chem. Soc.* **2016**, *138*, 6719−6722.

(9) Liang, J.; Li, J.; Yu, J.; Chen, P.; Fang, Q.; Sun, F.; Xu, R. $[(C_4H_{12}N)_2][Zn_3(HPO_3)_4]$: an Open-Framework Zinc Phosphite Containing Extra-Large 24-Ring Channels. *Angew. Chem., Int. Ed.* **2006**, *45*, 2546−2548.

(10) Huang, H.-L.; Wang, S.-L. An Extraordinary Boron-Mediated 16R-Channel-Containing Trivalent Vanadium Phosphite with Unique Solid State Redox Properties. *Chem. Commun.* **2010**, *46*, 6141−6143.

(11) Wang, K.; Bian, Y.; Li, J.; Xu, D.; Lin, Z. Amine-Ligated Approach for the Synthesis of Extra-Large-Pore Zinc Phosphites with qtz-h and bnn Topologies. *Inorg. Chem.* **2016**, *55*, 3727−3729.

(12) Yang, Y.; Li, N.; Song, H.; Wang, H.; Chen, W.; Xiang, S. Metal Phosphite Containing 24-Ring Channels with 10-Ring Windows. *Chem. Mater.* **2007**, *19*, 1889−1891.

(13) Lai, Y.-L.; Lii, K.-H.; Wang, S.-L. 26-Ring-Channel Structure Constructed from Bimetal Phosphite Helical Chains. *J. Am. Chem. Soc.* **2007**, *129*, 5350−5351.

(14) Lin, H.-Y.; Chin, C.-Y.; Huang, H.-L.; Huang, W.-Y.; Sie, M.-J.; Huang, L.-H.; Lee, Y.-H.; Lin, C.-H.; Lii, K.-H.; Bu, X.; Wang, S.-L. Crystalline Inorganic Frameworks with 56-Ring, 64-Ring, and 72-Ring Channels. *Science* **2013**, *339*, 811−813.

(15) Luo, X.; Luo, D.; Zeng, H.; Gong, M.; Chen, Y.; Lin, Z. A 3,4-Connected Beryllium Phosphite Framework Containing 24-Ring Channels with a Very Low Density. *Inorg. Chem.* **2011**, *50*, 8697−8699.

(16) Li, N.; Ma, Y.; Xiang, S.; Guan, N. Capturing an Aluminophosphite Intermediate in the New Route of Synthesizing Zeolite-Like Aluminophosphates. *Chem. Mater.* **2006**, *18*, 975−980.

(17) Lu, A.; Song, H.; Li, N.; Xiang, S.; Guan, N.; Wang, H. Novel Large Aluminophosphite Cage Unit as the Building Blocks to Form a Framework Structure Containing Multidimensional 12-Ring Channels. *Chem. Mater.* **2007**, *19*, 4142−4147.

(18) Morris, R. E.; Harrison, W. T. A.; Nicol, J. M.; Wilkinson, A. P.; Cheetham, A. K. Determination of Complex Structures by Combined Neutron and Synchrotron X-ray Powder Diffraction. *Nature* **1992**, *359*, 519−522.

(19) Morris, R. E.; Attfield, M. P.; Cheetham, A. K. Synthesis and Structures of Two Isostructural Phosphites, $Al_2(HPO_3)_3$ and $Ga_2(HPO_3)_3$. *Acta Crystallogr., Sect. C* **1994**, *50*, 473−476.

(20) Wang, L.; Song, T.; Fan, Y.; Wang, Y.; Xu, J.; Shi, S.; Zhu, T. $Ga_3(HPO_3)_4F_4(H_3DETA)$ (DETA = Diethylenetriamine): a New Open-Framework Fluorinated Gallium Phosphite with Pentameric Building Unit. *J. Solid State Chem.* **2006**, *179*, 824−829.

(21) Wang, L.; Song, T.; Fan, Y.; Tian, Z.; Wang, Y.; Shi, S.; Xu, J. Synthesis and Characterization of a New Open-Framework Fluorinated Gallium Phosphite with Three-Dimensional Intersecting Channels. *J. Solid State Chem.* **2006**, *179*, 3400−3405.

(22) Zhou, G.-P.; Yang, Y.-L.; Fan, R.-Q.; Xie, J.-Q.; Quan, X.-J. Hydrothermal Syntheses, Crystal Structures and Thermal Properties of Two New Organically Templated Open-Framework Gallium Phosphites. *Chem. Res. Chin. Univ.* **2013**, *29*, 201−205.

(23) Ramaswamy, P.; Mandal, S.; Natarajan, S. New Open-Framework Phosphate and Phosphite Compounds of Gallium. *Inorg. Chim. Acta* **2011**, *372*, 136−144.

(24) Huang, L.; Fan, Y.; Ma, H.; Li, C.; Wang, L. Synthesis and Characterizations of Two NbO Topological Gallium Phosphites with Low Framework Density. *Microporous Mesoporous Mater.* **2014**, *196*, 321−326.

(25) Huang, L.; Song, T.; Fan, Y.; Zhang, L.; Yang, H.; Tian, Z.; Wang, L. Synthesis, Characterization of a New Open-Framework Gallium Phosphite Containing 5,6-Fold Coordinate Gallium Atoms. *Inorg. Chim. Acta* **2009**, *362*, 3030−3034.

(26) Huang, L.; Song, T.; Zhang, L.; Chen, Y.; Jiang, J.; Xu, J.; Wang, L. Synthesis, Crystal Structure and Characterization of a New Layered Gallium Phosphite $Ga(HPO_3)F_3{\cdot}(trans\text{-}C_6N_2H_{16})$ with Left- and Right-Handed Helical Chains. *CrystEngComm* **2010**, *12*, 2198−2202.

(27) Huang, L.; Song, T.; Shi, S.; Tian, Z.; Wang, L.; Zhang, L. Hydrothermal Synthesis, Characterization, and Fluorescence Property of a Novel Layered Fluorinated Gallium Phosphite with Heptameric Building Unit. *J. Solid State Chem.* **2008**, *181*, 1279−1284.

(28) Morris, R. E.; Burton, A.; Bull, L. M.; Zones, S. I. SSZ-51−a New Aluminophosphate Zeotype: Synthesis, Crystal Structure, NMR, and Dehydration Properties. *Chem. Mater.* **2004**, *16*, 2844−2851.

DOI: 10.1021/acs.cgd.9b00725
Cryst. Growth Des. 2019, 19, 6011−6016

(29) Hua, W.; Chen, H.; Yu, Z.-B.; Zou, X.; Lin, J.; Sun, J. A Germanosilicate Structure with 11 × 11 × 12-Ring Channels Solved by Electron Crystallography. *Angew. Chem., Int. Ed.* **2014**, *53*, 5868−5871.
(30) Cichocka, M. O.; Lorgouilloux, Y.; Smeets, S.; Su, J.; Wan, W.; Caullet, P.; Bats, N.; McCusker, L. B.; Paillaud, J.-L.; Zou, X. Multidimensional Disorder in Zeolite IM-18 Revealed by Combining Transmission Electron Microscopy and X-Ray Powder Diffraction Analyses. *Cryst. Growth Des.* **2018**, *18*, 2441−2451.
(31) Lin, C.; Pan, F.; Li, J.; Chen, Y.; Shi, D.; Ma, T.; Yang, Y.; Du, X.; Wang, W.; Liao, F.; Lin, J.; Yang, T.; Sun, J. An Open-Framework Aluminophosphite with Face-Sharing AlO_6 Octahedra Dimers and Extra-Large 14-Ring Channels. *Cryst. Growth Des.* **2018**, *18*, 1267−1271.
(32) O'Keeffe, M.; Peskov, M. A.; Ramsden, S. J.; Yaghi, O. M. The Reticular Chemistry Structure Resource (RCSR) Database of, and Symbols for, Crystal Nets. *Acc. Chem. Res.* **2008**, *41*, 1782−1789.
(33) Eon, J.-G. Symmetry and Topology: the 11 Uninodal Planar Nets Revisited. *Symmetry* **2018**, *10*, 35−47.
(34) Murugavel, R.; Choudhury, A.; Walawalkar, M. G.; Pothiraja, R.; Rao, C. N. R. Metal Complexes of Organophosphate Esters and Open-Framework Metal Phosphates: Synthesis, Structure, Transformations, and Applications. *Chem. Rev.* **2008**, *108*, 3549−3655.
(35) Ma, Y.; Tong, W.; Zhou, H.; Suib, S. L. A Review of Zeolite-Like Porous Materials. *Microporous Mesoporous Mater.* **2000**, *37*, 243−252.
(36) Xu, R.; Pang, W.; Yu, J.; Huo, Q.; Chen, J. *Chemistry of Zeolites and Related Porous Materials: Synthesis and Structure*; Wiley, 2007; pp 19−116.
(37) Natarajan, S.; Mandal, S. Open-Framework Structures of Transition-Metal Compounds. *Angew. Chem., Int. Ed.* **2008**, *47*, 4798−4828.
(38) *Database of Zeolite Structures*; http://www.izastructure.org/databases/.
(39) Yu, J.; Xu, R. Rich Structure Chemistry in Aluminophosphate Family. *Acc. Chem. Res.* **2003**, *36*, 481−490.
(40) Sinnokrot, M. O.; Valeev, E. F.; Sherrill, C. D. Estimates of the Ab Initio Limit for π-π Interactions: the Benzene Dimer. *J. Am. Chem. Soc.* **2002**, *124*, 10887−10893.
(41) Lin, C.; Li, J.; Pan, F.; Zhao, Y.; Xu, L.; Yang, Y.; Du, X.; Lin, X.; Liao, F.; Lin, J.; Yang, T.; Sun, J. A Crystalline $AlPO_4$-5 Intermediate: Designed Synthesis, Structure, and Phase Transformation. *Dalton Trans* **2017**, *46*, 12209−12216.
(42) Guo, P.; Afeworki, M.; Cao, G.; Yun, Y.; Sun, J.; Su, J.; Wan, W.; Zou, X. Synthesis and Structure of a Layered Fluoroaluminophosphate and Its Transformation to a Three-Dimensional Zeotype Framework. *Inorg. Chem.* **2018**, *57*, 11753−11760.
(43) Li, N.; Xiang, S. Hydrothermal Synthesis and Crystal Structure of Two Novel Aluminophosphites Containing Infinite Al−O−Al Chains. *J. Mater. Chem.* **2002**, *12*, 1397−1400.
(44) Loiseau, T.; Riou, D.; Taulelle, F.; Férey, G. Synthesis and Characterization by X-Ray Diffraction and Solid State NMR of ULM-5, a New Fluorinated Gallophosphate $Ga_{16}(PO_4)_{14}(HPO_4)_2(OH)_2F_7\cdot 4H_3N(CH_2)_6NH_3\cdot 6H_2O$ with 16-Membered Rings. *Stud. Surf. Sci. Catal.* **1994**, *84*, 395−402.
(45) Sassoye, C.; Loiseau, T.; Taulelle, F.; Férey, G. A New Open-Framework Fluorinated Gallium Phosphate with Large 18-Ring Channels (MIL-31). *Chem. Commun.* **2000**, *11*, 943−944.
(46) Bonhomme, F.; Thoma, S. G.; Nenoff, T. M. A Linear DABCO Templated Fluorogallophosphate: Synthesis and Structure Determination from Powder Diffraction Data of $Ga(PO_4H)_2F\cdot[N_2C_6H_{14}]$. *J. Mater. Chem.* **2001**, *11*, 2559−2563.
(47) Gong, W.; Chu, D.; Jiang, H.; Chen, X.; Cui, Y.; Liu, Y. Permanent Porous Hydrogen-Bonded Frameworks with Two Types of Brønsted Acid Sites for Heterogeneous Asymmetric Catalysis. *Nat. Commun.* **2019**, 1 DOI: 10.1038/s41467-019-08416-6.
(48) Wang, H.; Li, B.; Wu, H.; Hu, T.-L.; Yao, Z.; Zhou, W.; Xiang, S.; Chen, B. A Flexible Microporous Hydrogen-Bonded Organic Framework for Gas Sorption and Separation. *J. Am. Chem. Soc.* **2015**, *137*, 9963−9970.

DOI: 10.1021/acs.cgd.9b00725
Cryst. Growth Des. 2019, 19, 6011−6016